Paleoceanography and Paleoclimatology

RESEARCH ARTICLE
10.1029/2019PA003655

Precession- and Obliquity-Induced Changes in Moisture Sources for Enhanced Precipitation Over the Mediterranean Sea

J.H.C. Bosmans[1,2], R.J. van der Ent[1,3], R.J. Haarsma[4], S.S. Drijfhout[4,5,6], and F.J. Hilgen[1]

[1]Faculty of Geosciences, Utrecht University, Utrecht, Netherlands, [2]Faculty of Science, Radboud University, Nijmegen, Netherlands, [3]Faculty of Civil Engineering and Geosciences, Delft University of Technology, Delft, Netherlands, [4]Royal Netherlands Meteorological Institute (KNMI), De Bilt, Netherlands, [5]Ocean and Earth Science, National Oceanography Centre, University of Southampton, Southampton, UK, [6]Faculty of Science, Utrecht University, Utrecht, Netherlands

Key Points:
- Moisture sources for precession-induced enhanced winter precipitation are local in fall and from the Atlantic in late winter
- For obliquity, precipitation changes are smaller; local and Atlantic sources play an equal role
- The Atlantic sources are not related to storm tracks but to low-latitude surface pressure changes

Supporting Information:
- Supporting Information S1

Correspondence to:
J. H. C. Bosmans,
Joyce.Bosmans@ru.nl

Citation:
Bosmans, J., vanderEnt, R. J., Haarmsa, R., Drijfhout, S. S., & Hilgen, F. J. (2020). Precession- and obliquity-induced changes in moisture sources for enhanced precipitation over the Mediterranean Sea. *Paleoceanography and Paleoclimatology*, *36*, e2019PA003655. https://doi.org/10.1029/2019PA003655

Received 9 MAY 2019
Accepted 9 JAN 2020
Accepted article online 10 JAN 2020

Abstract Enhanced winter precipitation over the Mediterranean Sea at times of minimum precession and maximum obliquity, that is, times of enhanced insolation seasonality, could provide freshwater required to form orbitally paced sedimentary cycles across the Mediterranean, offering a possible alternative to monsoonal runoff. We investigate the sources of the enhanced winter precipitation, by applying a moisture tracking model on the results of idealized orbital extreme experiments with a state-of-the-art climate model. Precession and obliquity enhance precipitation in fall and winter. Our study shows that the source of enhanced precipitation over the Mediterranean Sea differs during the winter half-year. In fall, the majority of the precession-induced precipitation increase originates from the Mediterranean itself. However, in late winter, the increase can be attributed to enhanced moisture advection from the Atlantic. This agrees with changes in evaporation and air-sea temperature differences over the Mediterranean. The obliquity-induced precipitation increase shows much less differences, with an equal contribution of local and Atlantic sources. The mechanism behind the Atlantic source of moisture, particularly important in late winter for precession-induced precipitation changes, is related to a weakened Azores High and slightly higher surface pressure over North Africa. The resulting anomalous circulation patterns generate enhanced Atlantic moisture transport toward the Mediterranean. These mechanisms coincide with weaker storm track activity over the North Atlantic, opposite to previous studies that often attribute enhanced Mediterranean winter precipitation to a southward shift and intensification of the Atlantic storm track. We thus provide an alternative mechanism for Atlantic sources of orbitally paced Mediterranean precipitation changes.

1. Introduction

Sedimentary cycles across the Mediterranean display 21,000- and 41,000-year precession and obliquity cycles, consistently indicating wetter conditions and lower surface water density during precession minima and obliquity maxima. The climatic origin of these cycles, including sapropels (or organic-rich layers) and carbonate cycles, is still debated after decades of research (e.g., Bosmans et al., 2015; Rohling et al., 2015). Wetter conditions over the Mediterranean and its borderlands are attributed to increases in winter precipitation (e.g., Milner et al., 2012; Toucanne et al., 2015; Tzedakis, 2009). Simultaneously, the North African monsoon and its runoff into the Mediterranean also intensify during precession minima and obliquity maxima (e.g., Bosmans et al., 2015a; Kutzbach et al., 2013). The latter is commonly held responsible for the formation of sapropels across the Mediterranean sea floor (e.g., Rohling et al., 2015; Rossignol-Strick, 1985; Ruddiman, 2007), with the runoff lowering surface water density and stagnating deep water formation, creating low-oxygen conditions. However, increased winter precipitation can be of the same order of magnitude as increased summer monsoon runoff (e.g., Bosmans et al., 2015; Simon et al., 2017) and may thus play a role as well. Furthermore, intermediate and deep water typically form in winter (Rohling et al., 2015, and references therein); therefore, increased winter precipitation may be more efficient in reducing the oxygenation of bottom waters than summer runoff.

The mechanisms behind orbitally induced variations in winter precipitation remain poorly understood, in contrast to the changes in orbitally forced changes in summer monsoon strength. Many studies attribute winter precipitation changes to storm track activity, which affects present-day winter precipitation and

can also explain consistent precipitation changes across the entire Mediterranean and its borderlands (e.g., Toucanne et al., 2015). Results of modeling studies do not yet show consensus. For instance, some find increased winter precipitation resulting from an intensification and southward shift of the Atlantic storm track during the early Holocene (Brayshaw et al., 2011) or at times of minimum precession (Kutzbach et al., 2013). By contrast, Bosmans et al. (2015) find reduced storm track activity over the North Atlantic during minimum precession and maximum obliquity, presumably as a consequence of a weakening in meridional temperature gradients. Instead of storm track activity, Bosmans et al. (2015) relate the enhanced precipitation during the winter half-year (October–March) in the Mediterranean area to an increased difference between air-sea temperatures, resulting in unstable conditions and locally generated convective precipitation.

Here, we aim to get a better understanding of the moisture sources and climate mechanisms behind the enigmatic changes in winter precipitation over the Mediterranean Sea for orbital extremes. We do so by looking in detail at bimonthly climate differences, rather than focusing on the mean of the winter half-year (Bosmans et al., 2015), and quantifying the moisture sources of the Mediterranean precipitation. For this reason, we apply the moisture tracking model WAM2 layers of van der Ent et al. (2014) to the output of the idealized precession and obliquity extreme runs of Bosmans et al. (2015) to quantify whether Mediterranean winter precipitation changes are indeed sourced locally. In section 2 we briefly repeat the model setup of the EC-Earth experiments from Bosmans et al. (2015) as well as describe the moisture tracking model WAM2 layers of van der Ent et al. (2014). Results are presented in section 3, followed by a discussion and conclusion in sections 4 and 5.

2. Methods

We use results from orbitally extreme experiments performed with the state-of-the-art climate model EC-Earth (e.g., Bosmans et al., 2015) as well as the WAM2 layers moisture tracking model (van der Ent et al., 2014).

2.1. The EC-Earth General Circulation Model

EC-Earth v2.2 is a state-of-the-art atmosphere-ocean general circulation model based on the operational seasonal forecast system of the European Centre for Medium-Range Weather Forecasts (Hazeleger et al., 2011). Using the climate model performance metric of Reichler and Kim (2008), Hazeleger et al. (2011) showed that EC-Earth stands out in its representation of circulation features and the vertical structure of the atmosphere. Furthermore, its resolution, interpolated from a spectral T159 grid to nominally $1.125 \times 1.125°$ in the atmosphere with 62 vertical levels and nominally 1° in the ocean with 42 vertical levels, is among the highest in models applied in paleoclimatology.

Here we use results of four orbital extreme experiments, which have previously been used to study precession- and obliquity-induced changes in monsoons as well as the Mediterranean freshwater budget (e.g., Bosmans, 2014; Bosmans et al., 2015). During a so-called precession minimum (Pmin), perihelion takes place at the summer solstice and therefore the Northern Hemisphere receives a relatively large amount of insolation. In winter, the Northern Hemisphere receives a relatively low amount of insolation because aphelion occurs at the winter solstice. This means that during minimum precession, the Northern Hemisphere insolation seasonality is enhanced. During precession maximum (Pmax), the insolation seasonality is decreased, because perihelion is reached during winter solstice and aphelion is reached during summer solstice. Both precession experiments are performed with high eccentricity, to strengthen the precession effect. The obliquity experiments are performed with a circular orbit, to single out the effect of obliquity. On the Northern Hemisphere, changes in obliquity (tilt of the Earth's rotational axis) have a similar but smaller impact as precession, with increased summer insolation and reduced winter insolation for increased obliquity. We refer to maximum obliquity (tilt) as Tmax and minimum obliquity as Tmin, following Tuenter et al. (2003), who uses the same orbital parameters. Note that for the Southern Hemisphere, the precession and obliquity effects are opposite (see, e.g., Bosmans et al., 2015, Figure 1).

To get a better understanding of the moisture sources that can explain orbitally forced changes in Mediterranean precipitation, we apply the offline Eulerian moisture tracking model WAM2 layers (see section 2.2) to the four orbital extreme experiments described in the previous paragraph (Bosmans et al., 2015). For this purpose, we take 12-hourly precipitation, evaporation, specific humidity, and wind, the latter two on 11 pressure levels, from EC-Earth from the last 30 years of the simulations.

2.2. The WAM2 Layer Moisture Tracking Model

The offline Eulerian moisture tracking model WAM2 layers of van der Ent et al. (2014); van der Ent (2014) tracks water precipitated over the Mediterranean Sea backward in time and space (t,x,y). The Mediterranean Sea is defined as all sea grid cells between the Strait of Gibraltar in the west and the Bosporus and the Suez Canal in the east. The model uses the following water balance equation:

$$\frac{\delta S_{M,k}}{\delta t} = \frac{\delta S_{M,k} u_k}{\delta x} + \frac{\delta S_{M,k} v_k}{\delta y} \pm F_{v,M} + P_k^M - E_{M,k} \tag{1}$$

where S_M denotes atmospheric moisture of Mediterranean precipitation origin (since we go back in time, precipitation is the source term), u is zonal wind speed, v is meridional wind speed, $F_{v,M}$ is the vertical flux of water of Mediterranean precipitation origin between the two layers which are considered in the tracking model, P^M is the precipitation over the Mediterranean Sea, E_M is the part of the evaporation that is of Mediterranean precipitation origin, the subscript k denotes the layer, which is either the upper or lower layer of the atmosphere. In general, $\frac{S_{M,k}}{S_k}$ is considered to be well mixed within a layer and grid cell.

The atmospheric moisture storage S_k is derived from EC-Earth's specific humidity at 11 pressure levels in the atmosphere and the surface pressure, whereby the boundary between the upper and lower layer is considered relative to the surface pressure so that it corresponds to approximately 2 km above the surface at standard sea level pressure. The horizontal fluxes $\frac{\delta S_{M,k} u_k}{\delta x}$ and $\frac{\delta S_{M,k} v_k}{\delta y}$ are based on the specific humidity and the wind speeds at 11 pressure levels in the atmosphere on which EC-Earth output is stored, the surface pressure, and the pressure at the boundary between the two layers. By applying a water balance without a vertical flux, comparing it to the instantaneous moisture storage values, we derive F_v as the closure term. P_k^M is distributed over the two atmospheric layers using a weighing determined by the vertical specific humidity profile and is by definition equal to 0 outside the Mediterranean Sea. $E_{M,k}$ is always 0 in the upper layer and leaves the atmosphere in the lower layer by

$$E_{M,lower} = \frac{S_{M,lower}}{S_M} \times E \tag{2}$$

The model is run in time steps of 15 min to ensure numerical stability. The 12-hourly accumulated fluxes P and E from EC-Earth are uniformly distributed, that is, constant, over the 12 hr, and the 12-hourly instantaneous humidity and wind values are linearly interpolated. We acknowledge that this is a simplification but consider it acceptable given that we are interested in climatic averages and large-scale patterns.

Using this model, we can calculate for each location globally the amount of evaporation contributing (now looking forward in time) to Mediterranean precipitation in a certain time period: E_M. We aggregate our results bimonthly and averaged over the full 30-year period for the four orbital extreme scenarios. The source area of all contributions to Mediterranean precipitation is termed the precipitationshed of the Mediterranean (Keys et al., 2012). A useful metric for the evaluation of regional versus regional sources of precipitation is the regional precipitation recycling ratio for the Mediterranean Sea, that is, the relative amount of precipitation that originates from Mediterranean evaporation:

$$\rho_r^M = \frac{\overline{E_M^M}}{\overline{P^M}} \tag{3}$$

where E_M^M is evaporation in the Mediterranean itself, which returns as precipitation over the Mediterranean, and P_M is all precipitation in the Mediterranean. The regional precipitation recycling ratio is always integrated over the entire Mediterranean Sea. Likewise, we can define the regional evaporation recycling ratio for the Mediterranean Sea, that is, the relative amount of evaporation raining back out over the Mediterranean:

$$\epsilon_r^M = \frac{\overline{E_M^M}}{\overline{E^M}} \tag{4}$$

where E^M is all evaporation from the Mediterranean and E^M_M is the part that recycles as in equation (3).

When comparing experiments to each other, we can consider a change in precipitation over the Mediterranean ΔP_M to consist of a change in Mediterranean recycling ΔE^M_M and external sources ΔE^M_e to the Mediterranean:

$$\Delta P_M = \Delta E^M_M + \Delta E^M_e \tag{5}$$

This allows us to quantify the share of the regional (i.e., Mediterranean) sources to total precipitation change, which we term the regional share of precipitation change:

$$\gamma^M_r = \frac{\Delta E^M_M}{\Delta P^M} = \frac{\rho^M_{r,exp2} \times P^M_{exp2} - \rho^M_{r,exp1} \times P^M_{exp1}}{P^M_{exp2} - P^M_{exp1}} = \frac{\epsilon^M_{r,exp2} \times E^M_{exp2} - \epsilon^M_{r,exp1} \times E^M_{exp1}}{P^M_{exp2} - P^M_{exp1}} \tag{6}$$

where subscript exp denotes experiment. We generally expect this metric to vary between 0 and 1, but note that this could theoretically be higher than 1, if, for example, Mediterranean precipitation increases and external sources decrease, or lower than 0, if Mediterranean precipitation increases and Mediterranean sources decrease.

3. Results

3.1. Bimonthly Climate Variability

Figures 1 and 2 show the bimonthly climate variability for precession and obliquity extremes, respectively. We interpret and discuss our results mainly in the light of the precipitation differences and their causes. These causes can either be found regionally over the Mediterranean or may be externally forced.

Figure 1a shows that precipitation and evaporation are overall high in winter, while summer is a dry season with low evaporation due to suppressing of evaporation by the vertical heat structure; sea surface temperatures are not much higher or even lower than air temperature (Figure 1b). In the minimum precession experiment (Pmin), precipitation over the Mediterranean Sea is increased during fall, winter, and early spring compared to maximum precession (Pmax), while precipitation is decreased in summer (Figure 1a). Changes in evaporation show a different pattern, with a strong increase in evaporation in Pmin in fall (September–October) but decreased evaporation for the rest of the year. This is a first indication that precipitation increases may be related to different mechanisms depending on the timing.

Furthermore, the sea-air temperature difference over the Mediterranean ($\Delta T = T_{seasurface} - T_{air}$, where we use $T2m$ as T_{air}) shows different behavior when comparing minimum and maximum precession (Figure 1b). While during Pmax $T_{seasurface}$ remains warmer than T_{air} in all months, during Pmin in summer T_{air} becomes warmer than $T_{seasurface}$ due to the strong increase in insolation, warming up the surrounding land faster than the sea surface (supporting information Figure S1, July–August). In fall, Pmin insolation drops below Pmax insolation, so the surrounding land and T_{air} decrease more strongly, while the lagged response of water temperature means $T_{seasurface}$ surface remains higher during Pmin (see Figure S1, September–October, showing temperatures over land decreasing while temperatures over the sea remain slightly higher). Therefore, $T_{seasurface}$ - T_{air} increases sharply, which coincides with the increased evaporation during fall. During Pmax, decreased insolation seasonality results in a lower seasonality in the sea-air temperature difference. The ΔT difference between Pmin and Pmax is more pronounced in fall than in winter and spring (see also Figure S1 for November–December and January–February).

The recycling ratios (equations (3) and (4)), resulting from the moisture tracking model, are shown in Figure 1c. The precipitation recycling ratio ρ_r (equation (3)) is overall lowest in spring and summer, when evaporation is low, indicating that the majority of moisture precipitating out over the Mediterranean Sea originates from outside the Mediterranean Sea. In fall and winter, when most precipitation occurs and evaporation is high, ρ_r increases to 0.4–0.45, indicating that 40–45% of the precipitation comes from Mediterranean Sea evaporation itself. From July–August to November–December, ρ_r for Pmin is higher than ρ_r for Pmax, while from January–February to May–June ρ_r for Pmin is lower. This already indicates that precipitation increases in fall are mainly locally sourced while precipitation increases in late winter are externally sourced. The evaporation recycling ratio ϵ_r (equation (4)) is overall low in summer, showing that of the low

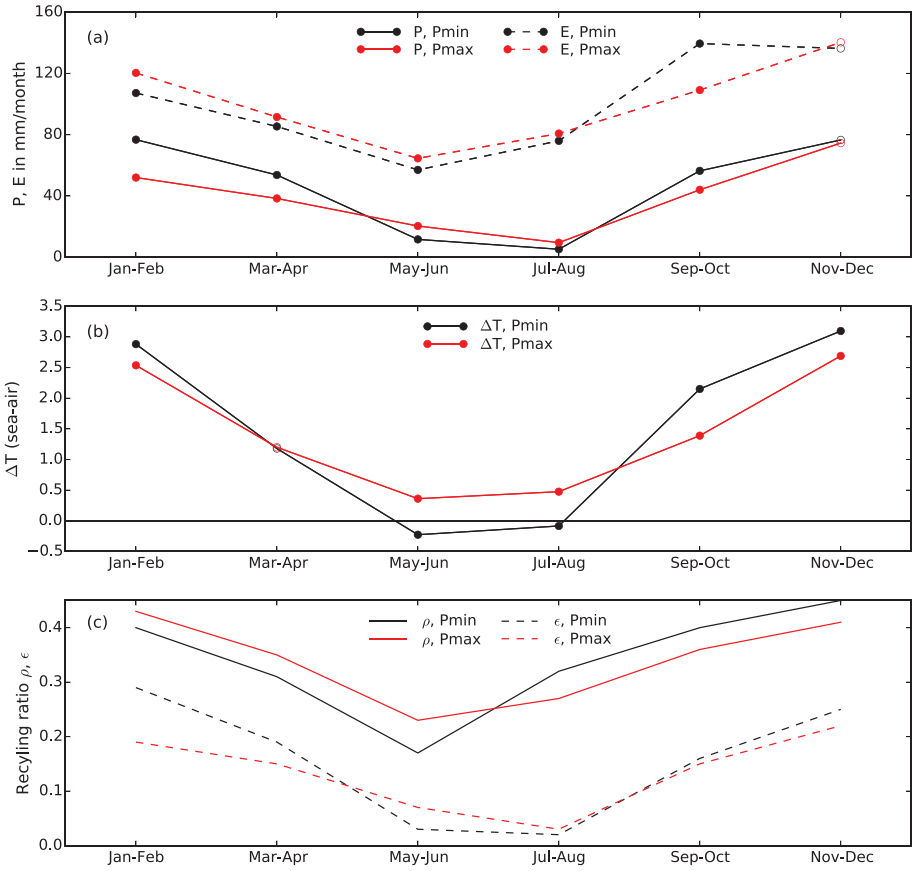

Figure 1. Precipitation and evaporation (P and E, a), sea-air temperature difference (T, b, expressed as the difference between sea surface temperature and 2-m air temperature), and the regional recycling ratios (ρ and ϵ, c) for precession minimum (Pmin, black) and maximum (Pmax, red) averaged bimonthly over the Mediterranean Sea. Precipitation, evaporation, and temperature are derived directly from EC-Earth GCM output; closed (open) dots indicate that the Pmin-Pmax difference is statistically significant (insignificant) at 95% using the two-sided Welch's t test on 30 years of bimonthly output. The recycling ratios (c) are derived through the WAM2 layers moisture tracking model. All values are 30-year averages.

amounts of evaporation, a relatively low amount rains out over the Mediterranean, as indicated by ρ_r as well. Higher values of ϵ_r in winter show that of the higher amounts of evaporation in winter, more rains out locally, as also indicated by ρ_r. However, the precession-induced changes in ϵ_r are different from changes in ρ_r, with ϵ_r being higher in Pmin throughout fall and winter, almost exactly following the changes in the sea-air temperature difference (Figure 1b).

Summarized for the precession-induced precipitation differences, we find that in fall and late winter precipitation is increased for Pmin. In fall (September–October), evaporation, the regional precipitation ratio ρ_r, and the regional evaporation recycling ratio ϵ_r are all increased, hence more evaporation of which a larger part rains out over the Mediterranean. Combined with the larger sea-air temperature difference, all model results indicate a stronger local mechanism behind the precipitation increases in September and October. The precipitation increases in late winter (January–February) on the other hand coincide with less evaporation, and a lower ρ_r for Pmin. Hence, precipitation is increased despite a relatively lower contribution of local evaporation. The sea-air temperature difference is still somewhat greater in Pmin compared to Pmax but the difference decreases. Overall these results indicate that in late winter, external causes play a stronger role in the precession-induced precipitation increase. We will look at the moisture sources and a quantification of local versus external causes of September–October and January–February precipitation differences (where the differences are strongest) in more detail in section 3.2.

For obliquity the results are shown in Figure 2. Precipitation is increased in fall and early winter during maximum obliquity (Tmax) compared to minimum obliquity (Tmin). The precipitation increase is highest in

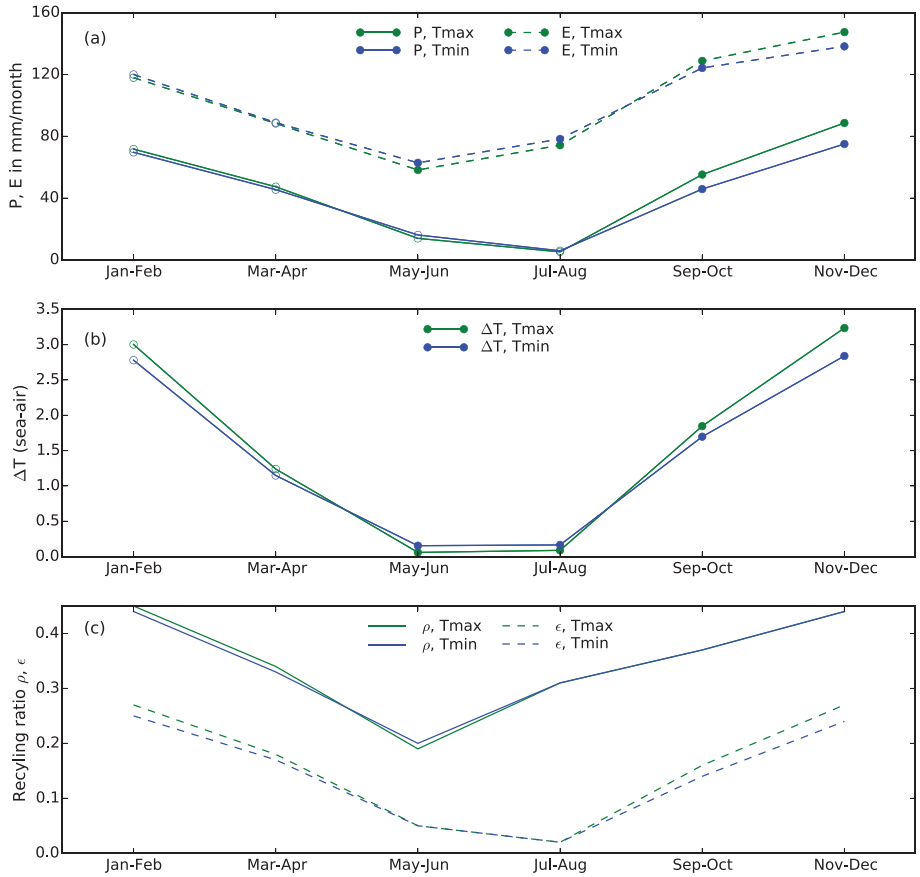

Figure 2. Precipitation and evaporation (P and E, a), sea-air temperature difference (T, b, expressed as the difference between sea surface temperature and 2-m air temperature), and the regional recycling ratios (ρ and ϵ, c) for obliquity maximum (Tmax, green) and minimum (Tmin, blue) averaged bimonthly over the Mediterranean Sea. Precipitation, evaporation, and temperature are derived directly from EC-Earth GCM output; closed (open) dots indicate that the Tmax-Tmin difference is statistically significant (insignificant) at 95% using the two-sided Welch's t test on 30 years of bimonthly output. The recycling ratios (c) are derived through the WAM2 layers moisture tracking model. All values are 30-year averages.

November–December, when it is accompanied by increased evaporation (Figure 2a). In late winter and early spring, obliquity-induced changes are not significant. As with Pmin, the increased seasonality of insolation during Tmax causes a sharper increase toward higher sea-air temperature differences in fall and early winter compared to Tmin (Figure 2b). In late winter ΔT is still higher during Tmax but the difference becomes insignificant. The seasonal pattern of ϵ_r coincides again with the seasonal pattern of ΔT, with higher values of ϵ_r for Tmax in fall and early winter (Figure 2c). The regional precipitation recycling ratio ρ_r is very similar between Tmax and Tmin. The recycling ratios for Tmax and Tmin show less difference than those of Pmin and Pmax (Figure 1c) as do the other variables, related to the smaller insolation differences.

The strongest precipitation differences for obliquity extremes are observed in November–December. Although the precipitation recycling ratio remains approximately equal, the absolute precipitation increase is seemingly related to a local feedback mechanism as it coincides with increased evaporation, an increased air-sea temperature difference and an increased evaporation recycling ratio. We will look at the moisture sources and a quantification of local versus external causes of November–December precipitation differences in more detail in section 3.2.

3.2. Moisture Sources

Figure 3 shows the moisture sources (E_M) of Mediterranean precipitation during the months where the differences in precipitation between the orbital extreme experiments are greatest. For all experiments and all months, the moisture sources show higher values in the western part of the Mediterranean compared to

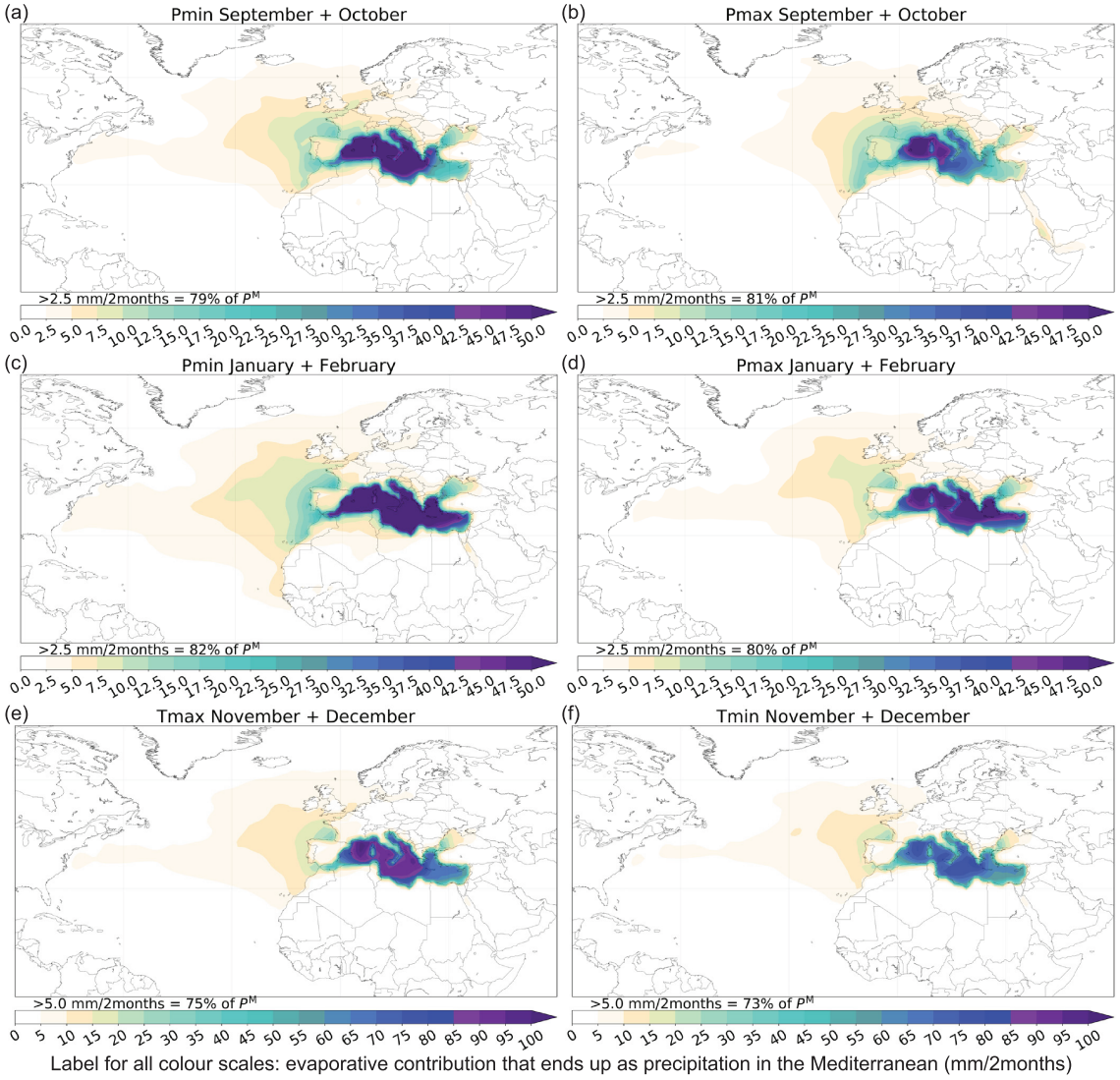

Figure 3. Precipitationsheds of Mediterranean Sea precipitation (i.e., the evaporative contribution E_M that ends up as precipitation over the Mediterranean Sea). The colors indicate how much evaporation from that location precipitates over the Mediterranean per 2 months. The percentages in the bottom left of the panels indicate how much of Mediterranean precipitation is contributed by all colored areas (i.e., contributions of more than 2.5 mm per 2 months for panels a–d and 5 mm per 2 months for panels e and f). The titles of the individual panels indicate the experiments and the months. The panels on the left show the experiments that receive more precipitation (Pmin, Tmax), and the panels on the right show the same months for the experiments that receive less precipitation (Pmax, Tmin).

the eastern part as well as a source area extending into the Atlantic Ocean. The shapes of the precipitationsheds (source areas) are consistent with the prevailing wind patterns and in line with studies for present-day climate (e.g., Schicker et al., 2010). Figure 4 shows how these precipitationsheds change in absolute and relative terms for the same months. The three cases of Figures 3 and 4 are summarized in Table 1.

In September–October, at the beginning of the rainy winter season, the Pmin experiment has more precipitation compared to Pmax as well as more evaporation and higher precipitation and evaporation recycling ratios (Figure 1 and Table 1). The moisture sources of Pmin (Figure 3a) and Pmax (Figure 3b) during September–October both show a sharp contrast in E_M at the sea-land boundary, with the sea contribution logically being much greater. While the shape of the precipitationsheds in Figures 3a and 3b is similar, the absolute values are not. E_M is higher over the Mediterranean, and there is a strong increase in local evaporation contribution for Pmin compared to Pmax (Figures 4a and 4b). The precipitation increase is mostly due to Mediterranean sources (regional share of precipitation change $\gamma_r^M = 0.54$, Table 1), the nearby Atlantic contribution (from coastal Morocco and the Iberian peninsula) even decreases (Figures 4a and 4b). The

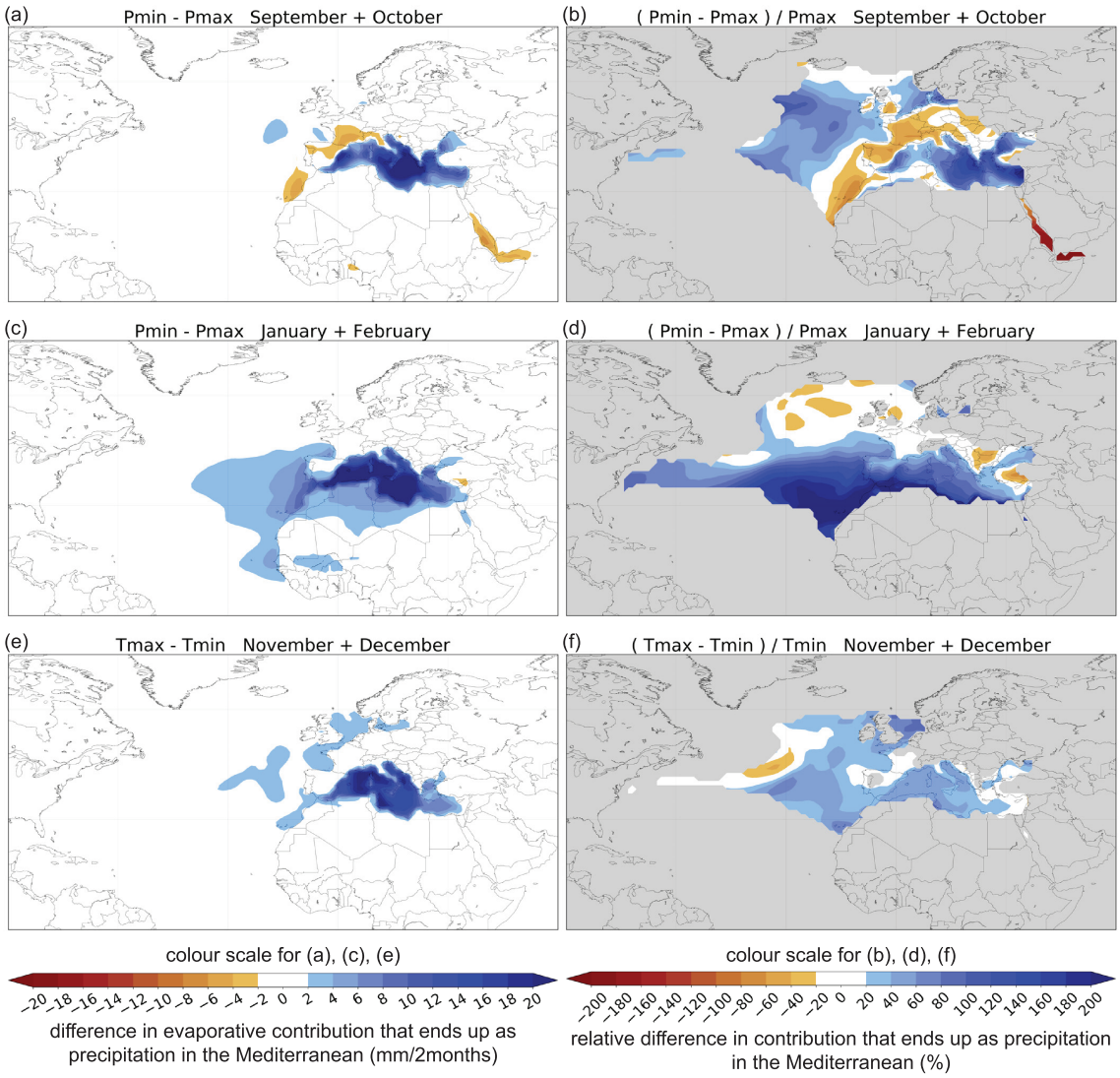

Figure 4. Precipitationshed (E_M) differences of Mediterranean Sea precipitation. Panels (a), (c), and (e) are computed by substracting Figure 3b − Figure 3a, Figure 3d − Figure 3c, and Figure 3f − Figure 3e, respectively. Panels (b), (d), and (f) are the relative values (left figure divided by E_{MPmax} or E_{MTmin}). In the panels on the right of this figure, the areas that do not pass the colored contribution threshold in any of the two companion panels of Figure 3 are masked gray (E_M per 2 months less than 2.5 mm/day for precession and d and 5 mm/day for obliquity).

moisture sources analysis thus suggests that the main mechanism behind the enhanced precipitation in September–October is increased local convection, which is in line with Bosmans et al. (2015). This is also in line with present-day studies suggesting that increased sea surface temperatures lead to more extreme precipitation in fall (e.g., Millán, 2014).

Comparing Figure 3c to Figure 3d shows that the increase in precipitation for Pmin in January–February is associated with both stronger contributions from local sources as well as stronger contributions from the Atlantic (see Figures 4c and 4d). The source areas (Figures 3c and 3d) extend further (south)west on the Atlantic Ocean. March–April exhibit similar results (not shown). Although the evaporation recycling ratio ϵ_r^M is increased and the sea-air temperature difference is bigger for Pmin in January–February, the total Mediterranean evaporation is decreased as is ρ_r^M (Table 1). Combined, we find that roughly one third of the precipitation increase is due to local moisture sources ($\gamma_r^M = 0.34$, Table 1); therefore, the Atlantic is the main source and the most likely driver behind the increased precipitation in January–February.

The increase in winter precipitation for Tmax compared to Tmin is strongest in November–December. Figures 3e and 3f show the moisture sources for precipitation in this month for both experiments. The shape

Table 1
Different Cases of Increased Precipitation in the Orbital Extreme Scenarios

Case	Pmin-Pmax September–October	Pmin-Pmax January–February	Tmax-Tmin November–December
P (mm/month)	44 (Pmax)	52 (Pmax)	75 (Tmin)
ΔP (mm/month)	12	25	14
E (mm/month)	109 (Pmax)	120 (Pmax)	138 (Tmin)
ΔE (mm/month)	30	−13	9
$T_{sea-air}$ (°)	1.4 (Pmax)	2.5 (Pmax)	2.8 (Tmin)
$\Delta T_{sea-air}$ (°)	0.8	0.35	0.4
ϵ_r^M	0.15 (Pmax)	0.19 (Pmax)	0.19 (Tmin)
$\Delta\epsilon_r^M$	0.02	0.10	0.03
ρ_r^M	0.36 (Pmax)	0.43 (Pmax)	0.44 (Tmin)
$\Delta\rho_r^M$	0.04	-0.03	0.00
γ_r^M	**0.54**	**0.34**	**0.46**

Note. The regional share of precipitation change (γ_r^M) highlights the importance of the Mediterranean versus external sources of increased precipitation and is shown in bold.

is again very similar, but both the local sources and sources from the eastern Atlantic are somewhat amplified (Figures 4e and 4f). Table 1 shows that local evaporation is higher in Tmax compared to Tmin, in line with a higher $\Delta T_{air-sea}$. The regional share of precipitation change (γ_r^M) is 0.46, with relatively small changes in ϵ_r^M and no change in ρ_r^M. We therefore conclude that the cause of the precipitation increase during Tmax in November–December is a mixture of local and external processes.

3.3. Mechanisms Behind Atlantic Moisture Sources

So far, we have quantified the relative roles of Mediterranean and external/Atlantic moisture sources contributing to precession- and obliquity-induced differences in precipitation over the Mediterranean Sea. For precession-induced precipitation changes in fall, we identified that the moisture sources are mainly local. This matches our earlier conclusions in Bosmans et al. (2015) where we attributed enhanced winter precipitation to increased sea-air temperature differences over the Mediterranean rather than storm track activity over the Atlantic. However, looking in higher temporal resolution and adding a moisture tracking model, we now find that in late winter, the majority of the precipitation increase originates from remote, Atlantic, sources, as does half the obliquity-induced precipitation increase in early winter.

This raises the question of what drives the changes in remote, Atlantic, sources and whether this mechanism changes seasonally as well. We therefore look at bimonthly rather than October–March averaged storm track activity and moisture transport from the EC-Earth simulations, see Figure 5 and Table 1. In fall (September–October), storm track activity is increased over the North Atlantic along with increased westerly moisture transport into Europe (Figures 5a and 5b). Over the Mediterranean there is a slight increase in storm track activity, while net precipitation *P-E* is reduced (Figure 5b). The latter reflects the stronger increase in evaporation than in precipitation (Figure 1a), which agrees with a local source of increased precipitation. In late winter (January–February), storm track activity over the North Atlantic is decreased (Figure 5c), as is westerly moisture transport into Europe. Over the Mediterranean, net precipitation is higher (Figure 5d), reflecting the coincidence of increased precipitation and decreased evaporation in late winter (Figure 1a). Figure 5d furthermore shows that there is increased moisture transport from (or reduced moisture export to) the Atlantic, particularly near the Iberian/Moroccan coast, toward the Mediterranean. The latter explains the external source of increased Mediterranean precipitation. For obliquity, storm track activity in November–December is largely decreased in Tmax compared to Tmin, with some increases just south of the Mediterranean and further west over the Atlantic (Figure 5e). There is little change in moisture transport and net precipitation is slightly increased (Figure 5f).

The mechanism behind the externally driven moisture source of precession-induced precipitation increase in January–February can be further explained by looking at changes in pressure, wind, and temperature. The surface wind anomaly shows a cyclonic pattern around a low-pressure anomaly, indicating a weakened Azores High pressure area with a weakened anticyclonic (clockwise) circulation (Figure 6a), including anomalous winds toward the Mediterranean along the southern edge of the pressure anomaly. The latter

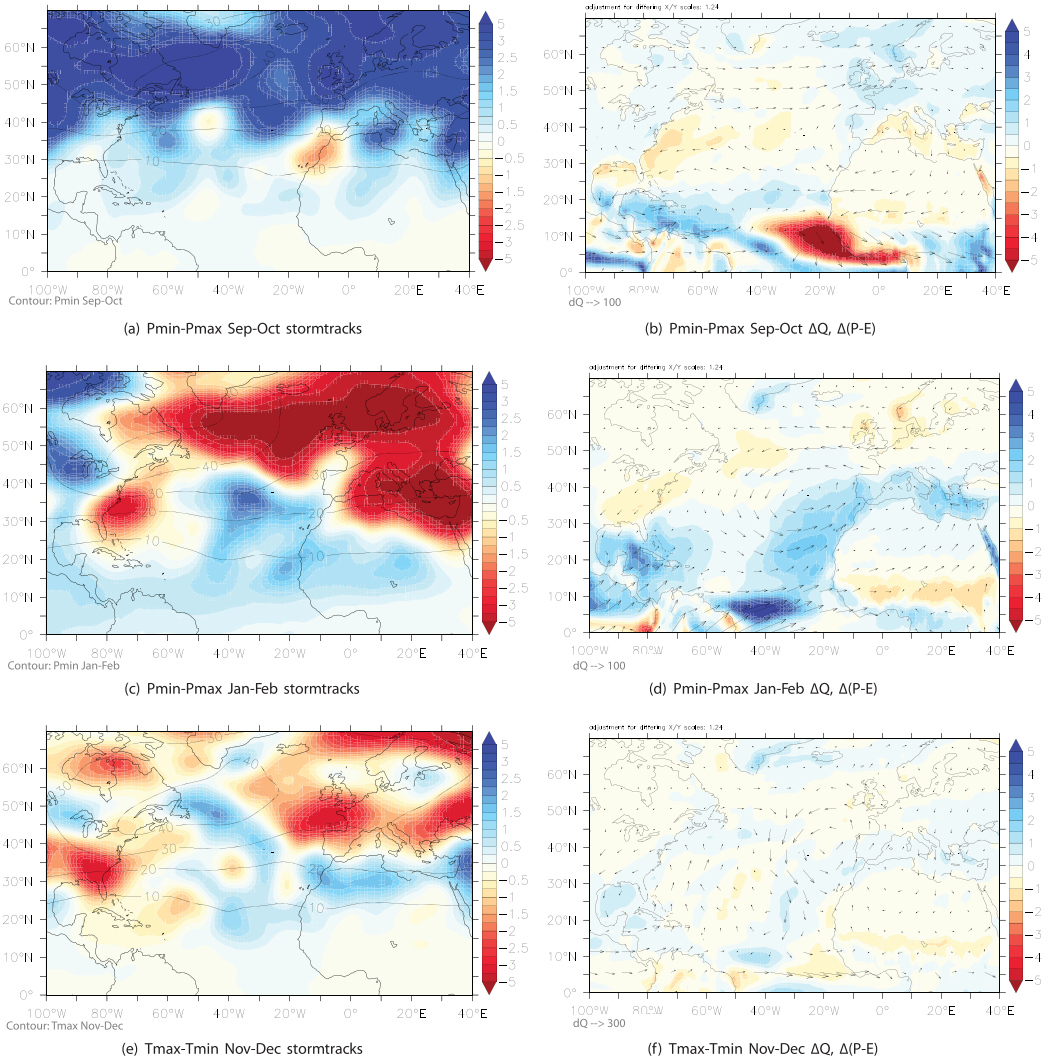

Figure 5. Storm track activity on the left (a, c, and e, in m) based on the 500-hPa geopotential height standard deviation, filtered for 2.5–8 days (see Bosmans et al., 2015). Changes in vertically integrated moisture transport *Q* and net precipitation *P-E* on the right (b, d, f, in kg/(ms) and mm/day) (see Bosmans et al., 2015a, for a definition of *Q*). (a, b) Precession-induced difference in September–October. (c, d) Precession-induced difference in January–February. (e, f) Obliquity-induced difference in November–December. Contours are the absolute storm track activity in Pmin or Tmax.

coincides with the slight increase in storm track activity near the Iberian/Moroccan coast (Figure 5c). The cyclonic wind pattern is consistent in height (see wind anomaly at 850 hPa—roughly 1.5-km height—in Figure 6b), consistent with the moisture transport anomaly (Figure 5d). A slight increase in pressure over tropical North Africa further strengthens the wind and moisture transport into the Mediterranean across the Iberian/Moroccan coasts. This pressure increase is linked to a strong decrease in surface temperature over tropical North Africa (supporting information Figure S1d). A similar change in surface pressure and wind can be seen for obliquity in November–December (supporting information Figure S2); hence, the same mechanisms may explain the obliquity-induced externally driven precipitation changes. We furthermore note that the changes in moisture transport are mainly due to changes in mean flow, the eddy term which would change due to storm tracks is small (supporting information Figure S3).

For precession, the weaker anticyclonic (clockwise) circulation around the weakened Azores High can explain the small temperature decrease off the Iberian coast, as southward winds from colder latitudes are reduced, while further west weaker northward winds can explain the stronger decrease in surface temperatures (supporting information Figure S1d). The weakened Azores High itself could be related to a weaker monsoon circulation over South America, caused by the reduced January–February insolation during Pmin.

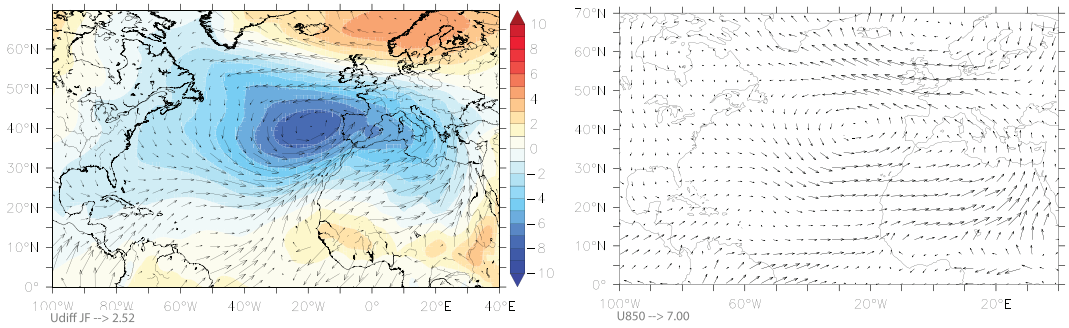

(a) Pmin-Pmax Jan-Feb SLP, wind (b) Pmin-Pmax Jan-Feb 850 hPa wind

Figure 6. Precession-induced changes in (a) sea level pressure (SLP, hPa) and surface wind (at 10 m) as well as (b) wind at 850 hPa during January–February.

As the monsoon can be considered part of the Hadley circulation, a weaker monsoon coincides with weaker upward air motion in the Hadley circulation's rising branch. As a response, the descending branch reaches less far north during Pmin, resulting in a reduction of downward air motion over the Azores High, which weakens as a result (Figure 7). In this respect, the late winter situation is remarkably opposite from that observed during late summer when the Azores High is strengthened with a strengthening of the trade winds during Pmin (Figures 7 and 8 in Bosmans et al., 2015a).

We thus find that changes in storm track activity and moisture transport toward the Mediterranean vary within the winter half-year. For precession, precipitation increases are mainly local in September–October and mainly external in January–February. The mechanism behind the external moisture sources is not related to storm tracks but to reduced sea level pressure at the Azores High, with a corresponding wind and moisture transport anomaly toward the Mediterranean from the subtropical Atlantic. For obliquity, where we showed that precipitation increases are equally attributable to local and remote sources, we see overall smaller storm track activity and little change in moisture transport.

4. Discussion

In this study, we uncover more temporal detail in the discussion on the moisture source of orbitally forced enhanced Mediterranean winter precipitation, using both the EC-Earth GCM and the WAM2 layers moisture tracking model, showing that both local and nonlocal processes can play a role, depending on the season or months under investigation. Here we place our findings within the context of literature on orbitally forced winter precipitation changes, as an alternative source of freshwater for sapropel formation besides summer

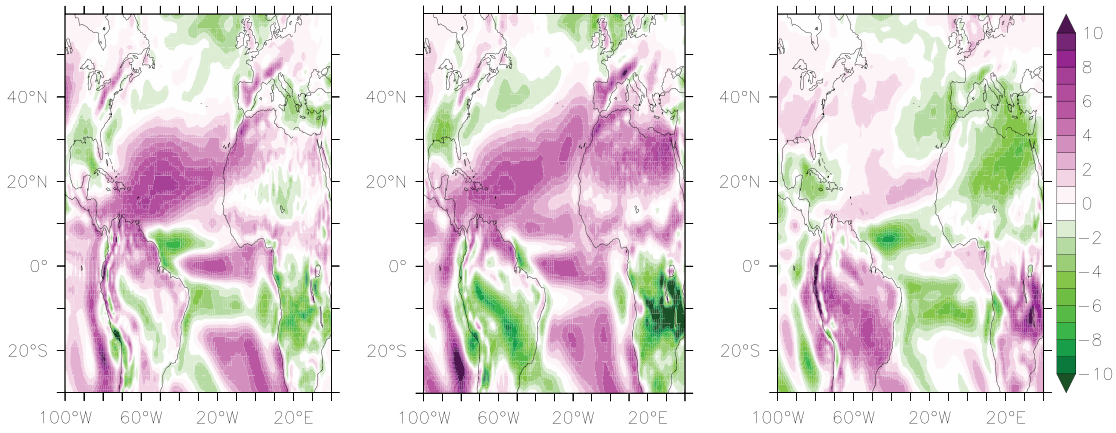

Figure 7. Vertical velocity W at 500 hPa (5-km height) in 10^{-2} Pa/s for Pmin (left), Pmax (middle), and the Pmin-Pmax difference for January–February. Positive values (purple) indicate downward motion, negative values (green) indicate upward motion.

monsoon runoff (Bosmans et al., 2015a; Rossignol-Strick, 1985; Ruddiman, 2007) and discuss limitations of our study and suggestions for further research.

4.1. The Role of the Atlantic in Orbitally Paced Mediterranean Sedimentary Cycles

Looking at bimonthly differences in this study revealed that Mediterranean and Atlantic moisture sources are both responsible for Mediterranean precession- and obliquity-induced winter precipitation increases, with their relative roles varying throughout the seasons. Local (Mediterranean) mechanisms, which are the main factor in fall for precession, are in line with our earlier suggestion that changes in air-sea temperature differences play a critical role (Bosmans et al., 2015). Furthermore, we now acknowledge that external, that is, Atlantic, moisture sources also contribute to the Mediterranean freshwater budget on orbital time scales. These are related to changes in the Azores High with corresponding changes in wind and moisture transport. Importantly, neither local nor external mechanisms seem to be related to changes in North Atlantic storm tracks as suggested in earlier studies (e.g., Kutzbach et al., 2013; Toucanne et al., 2015). Such external sources could be important for sapropel formation, as external sources are most important in late winter when deep water formation occurs (e.g., Rohling et al., 2015).

Furthermore, the mechanism behind the Atlantic moisture sources also explains the enhanced winter precipitation along the Atlantic margin of the Mediterranean (shown in Bosmans et al., 2015). This enhanced precipitation is likely responsible for the carbonate dilution cycles, which are formed in-phase with precession, of late Miocene to late Pleistocene age deposited along this margin (Sierro et al., 2000; van der Laan et al., 2012; Van den Berg et al., 2015), and possibly also in the western basin of the Mediterranean (Ochoa et al., 2018). Related cycles are also found northward up to the Iberian margin (Hodell et al., 2013), showing a distribution that corresponds very well with the enhanced winter precipitation in our model output. Such studies suggest that a similar mechanism exists behind orbitally paced sedimentary cycles in the Mediterranean as well as the Iberian margin. Our study adds the insight that the late winter Atlantic moisture sources are related to low-latitude mechanisms rather than storm tracks. However, a contribution of the monsoon in summer cannot be fully excluded, particularly for sedimentary cycles along the Moroccan coast, as monsoonal precipitation may reach the tip of NW Africa in late summer during Pmin (Bosmans et al., 2015a).

Our low-latitude mechanisms for the Atlantic moisture sources are different from those previously suggested in paleomodeling literature. Increases or shifts in the Atlantic storm track as well as storm track activity over the Mediterranean have been invoked, with increased Mediterranean storm track activity found for the Early Holocene (Brayshaw et al., 2011) and for minimum precession by Kutzbach et al. (2013). On the other hand, Kaspar et al. (2007) found weakened Mediterranean storm tracks during the Eemian, a period of high-amplitude minimum precession. Differences in these findings could be related to differences in model setup, parameterization, and resolution (Bosmans et al., 2015). Verifying which of these model differences causes the variations in reported mechanisms for precipitation changes is beyond the scope of this study. Nonetheless, based on EC-Earth's skill in atmospheric circulation features as well as its high resolution compared to other paleomodel studies (see section 2.1; Hazeleger et al., 2011; Reichler & Kim, 2008), we believe that EC-Earth may be better capable in capturing the storm tracks than other models applied in such studies.

4.2. Limitations and Suggestions for Further Research

Despite uncovering more temporal detail and suggesting new mechanisms for Atlantic moisture sources in orbitally induced Mediterranean precipitation changes, our study has its limitations. We base our results on idealized precession and obliquity extreme simulations, whereas orbital configurations outside of orbital extremes or transient simulations can shed more light on the temporal development of sapropels and could explain why some sapropels are better developed than others (e.g., Grant et al., 2016; Marzocchi et al., 2015).

Furthermore, in our moisture tracking computations, we use precipitation over the entire Mediterranean Sea as a sink, from which moisture is tracked backwards. This means we made the simplified assumption that precipitation changes affect deep water formation similarly across the basin. Although Rohling et al. (2015) suggest that sapropels (or Organic Rich Layers) in the eastern and western Mediterranean are mechanistically similar, with sapropels in the east being better developed due to a higher sensitivity to developing deep-sea anoxia, they also note that in each sapropel episode the environmental paramaters can vary over space and time. Within the basin, particularly the locally driven precipitation changes can affect salinity

gradients. Applying the moisture tracking model over subregions rather than the entire Mediterranean Sea could help further disentangle mechanisms for shifts in the hydrological budget over the area.

Lastly, we ignore other factors that could precondition the Mediterranean Sea for deep-sea anoxia, such as sea level changes, sea water temperature changes, or meltwater addition (e.g., Grant et al., 2016; Grimm et al., 2015; Rohling et al., 2015).

Besides further research into the mechanisms behind precipitation changes at other orbital configurations and over regions within the Mediterranean Sea, another question that remains is which precipitation source is ultimately responsible for reduced deep water formation and thus sapropel formation. Forcing a Mediterranean ocean circulation model with the separate and combined changes in summer monsoon runoff, fall and late winter precipitation can reveal whether one of these sources separately is sufficient, or whether all sources are needed to (pre)condition the basin for reduced deep water formation.

5. Conclusion

In this study we apply for the first time a moisture tracking model to the results of idealized precession and obliquity simulations of a state-of-the-art GCM. By investigating bimonthly precipitation, evaporation, and moisture recycling ratios, we find that the mechanisms behind precipitation changes over the Mediterranean Sea, which may ultimately lead to sapropel formation, vary throughout the seasons. For precession, local mechanisms related to a strong air-sea temperature difference dominate precipitation changes in fall, while later in winter precipitation changes are dominated by external moisture sources. For obliquity, precipitation changes are smaller and attributed equally to local and external sources. The external moisture sources from the Atlantic are related to circulation changes in response to a reduced Azores high pressure area and slightly higher pressure over tropical North Africa. We thus propose both local as well as Atlantic mechanisms for orbitally paced changes in Mediterranean precipitation alternative to previously proposed changes in storm track activity.

Acknowledgments
The authors thank two anonymous reviewers for their comments, which helped to improve the manuscript. The EC-Earth simulations were performed as part of J. H. C. Bosmans' PhD project within Utrecht University's "Focus en Massa" call. Modeling support was provided by the Royal Netherlands Meteorological Institute (KNMI) and the European Centre for Medium-Range Weather Forecast (ECMWF). The WAM2 layer simulations were performed at the Cartesius SurfSara supercomputing facilities. Details on the EC-Earth setup and orbital forcing can be found in Bosmans (2014). The climatological monthly mean output of the simulations is available through Zenodo: Bosmans (2019). Idealized orbital extreme GCM simulations with EC-Earth-2-2 [Data set]. Zenodo (http://doi.org/10.5281/zenodo.3268528). Higher temporal resolution output (12-hourly or daily) can be obtained from the lead author. The WAM2 layer model code (van der Ent, 2014; van der Ent et al., 2014) is available for download at: van der Ent, R. J.: WAM2layersPython (https://github.com/ruudvdent/WAM2layersPython), last access: 23 November 2016.

References

Bosmans, J. (2014). A model perspective on orbital forcing of monsoons and Mediterranean climate using EC-Earth. Utrecht University, Depts. of Physical Geography and Earth Sciences.

Bosmans, J. (2019). Idealized orbital extreme GCM simulations with EC- Earth-2-2. Zenodo. https://doi.org/10.5281/zenodo.3268528

Bosmans, J., Drijfhout, S., Tuenter, E., Hilgen, F., & Lourens, L. (2015a). Response of the north african summer monsoon to precession and obliquity forcings in the EC-Earth GCM. *Climate Dynamics*, *44*(1-2), 279–297.

Bosmans, J., Drijfhout, S., Tuenter, E., Hilgen, F., Lourens, L. J., & Rohling, E. (2015). Precession and obliquity forcing of the freshwater budget over the Mediterranean. *Quaternary Science Reviews*, *123*, 16–30.

Brayshaw, D. J., Rambeau, C. M. C., & Smith, S. J. (2011). Changes in Mediterranean climate during the Holocene: Insight from global and regional climate modelling. *The Holocene*, *21*(1), 15–31. https://doi.org/10.1177/0959683610377528

Grant, K., Grimm, R., Mikolajewicz, U., Marino, G., Ziegler, M., & Rohling, E. (2016). The timing of Mediterranean sapropel deposition relative to insolation, sea-level and african monsoon changes. *Quaternary Science Reviews*, *140*, 125–141.

Grimm, R., Maier-Reimer, E., Mikolajewicz, U., Schmiedl, G., Müller-Navarra, K., Adloff, F., et al. (2015). Late glacial initiation of holocene eastern Mediterranean sapropel formation. *Nature Communications*, *6*, 7099.

Hazeleger, W., Wang, X., Severijns, C., Stefanescu, S., Bintanja, R., Sterl, A., et al. (2011). EC-Earth V2.2: Description and validation of a new seamless Earth system prediction model. *Climate Dynamics*, *39*, 1–19. https://doi.org/10.1007/s00382-011-1228-5

Hodell, D., Crowhurst, S., Skinner, L., Tzedakis, P. C., Margari, V., Channell, J. E., et al. (2013). Response of Iberian Margin sediments to orbital and suborbital forcing over the past 420 ka. *Paleoceanography*, *28*(1), 185–199.

Kaspar, F., Spangehl, T., & Cubasch, U. (2007). Northern hemisphere winter storm tracks of the Eemain interglacial and the last glacial inception. *Climate of the Past*, *3*, 181–192.

Keys, P. W., van der Ent, R. J., Gordon, L. J., Hoff, H., Nikoli, R., & Savenije, H. H. G. (2012). Analyzing precipitationsheds to understand the vulnerability of rainfall dependent regions. *Biogeosciences*, *9*(2), 733–746. https://doi.org/10.5194/bg-9-733-2012

Kutzbach, J. E., Chen, G., Cheng, H., Edwards, R. L., & Liu, Z. (2013). Potential role of winter rainfall in explaining increased moisture in the Mediterranean and Middle East during periods of maximum orbitally-forced insolation seasonality. *Climate Dynamics*, *42*, 1079–1095. https://doi.org/10.1007/s00382-013-1692-1

Marzocchi, A., Lunt, D., Flecker, R., Bradshaw, C., Farnsworth, A., & Hilgen, F. (2015). Orbital control on late Miocene climate and the North African monsoon: Insight from an ensemble of sub-precessional simulations. *Climate of the Past*, *11*(10), 1271–1295.

Millán, M. M. (2014). Extreme hydrometeorological events and climate change predictions in Europe. *Journal of Hydrology*, *518*, 206–224.

Milner, A. M., Collier, R. E., Roucoux, K. H., Müller, U. C., Pross, J., Kalaitzidis, S., et al. (2012). Enhanced seasonality of precipitation in the Mediterranean during the early part of the last interglacial. *Geology*, *40*(10), 919–922.

Ochoa, D., Sierro, F. J., Hilgen, F. J., Cortina, A., Lofi, J., Kouwenhoven, T., & Flores, J.-A. (2018). Origin and implications of orbital-induced sedimentary cyclicity in pliocene well-logs of the western Mediterranean. *Marine Geology*, *403*, 150–164.

Reichler, T., & Kim, J. (2008). How well do coupled models simulate today's climate? *Bulletin of the American Meteorological Society*, *89*(3), 303–312.

Rohling, E., Marino, G., & Grant, K. (2015). Mediterranean climate and oceanography, and the periodic development of anoxic events (sapropels). *Earth-Science Reviews*, *143*, 62–97.

Rossignol-Strick, M. (1985). Mediterranean Quaternary sapropels, an immediate response of the African monsoon to variation of insolation. *Palaeogeography, Palaeoclimatology, Palaeoecology*, *49*, 237–263.

Ruddiman, W. F. (2007). *Earth's climate: Past and future*. New York: W.H. Freeman. http://books.google.nl/books?id=Mpj_GwAACAAJ

Schicker, I., Radanovics, S., & Seibert, P. (2010). Origin and transport of Mediterranean moisture and air. *Atmospheric Chemistry and Physics*, *10*(11), 5089–5105. https://doi.org/10.5194/acp-10-5089-2010

Sierro, F. J., Ledesma, S., Flores, J. A., Torrescusa, S., & Martinez del Olmo, W. (2000). Sonic and gamma-ray astrochronology: Cycle to cycle calibration of atlantic climatic records to Mediterranean sapropels and astronomical oscillations. *Geology*, *28*, 695–698.

Simon, D., Marzocchi, A., Flecker, R., Lunt, D. J., Hilgen, F. J., & Meijer, P. T. (2017). Quantifying the Mediterranean freshwater budget throughout the late miocene: New implications for sapropel formation and the Messinian salinity crisis. *Earth and Planetary Science Letters*, *472*, 25–37.

Toucanne, S., Minto'o, C. M. A., Fontanier, C., Bassetti, M.-A., Jorry, S. J., & Jouet, G. (2015). Tracking rainfall in the northern Mediterranean borderlands during sapropel deposition. *Quaternary Science Reviews*, *129*, 178–195.

Tuenter, E., Weber, S. L., Hilgen, F. J., & Lourens, L. J. (2003). The response of the African summer monsoon to remote and local forcing due to precession and obliquity. *Global and Planetary Change*, *36*, 219–235. https://doi.org/10.1016/S0921-8181(02)00196-0

Tzedakis, P. (2009). Cenozoic climate and vegetation change, *The physical geography of the Mediterranean* pp. 89–137). Oxford: Oxford University Press.

Van den Berg, B., Sierro, F., Hilgen, F., Flecker, R., Larrasoaña, J., Krijgsman, W., et al. (2015). Astronomical tuning for the upper Messinian spanish atlantic margin: Disentangling basin evolution, climate cyclicity and MOW. *Global and Planetary Change*, *135*, 89–103.

van der Ent, R. J. (2014). A new view on the hydrological cycle over continents (Ph.D.), Delft University of Technology. https://doi.org/10.4233/uuid:0ab824ee-6956-4cc3-b530-3245ab4f32be

van der Ent, R. J., Wang-Erlandsson, L., Keys, P. W., & Savenije, H. HG (2014). Contrasting roles of interception and transpiration in the hydrological cycle—Part 2: Moisture recycling. *Earth System Dynamics*, *5*(2), 471–489.

van der Laan, E., Hilgen, F. J., Lourens, L. J., de Kaenel, E., Gaboardi, S., & Iaccarino, S. (2012). Astronomical forcing of northwest African climate and glacial history during the late Messinian (6.5-5.5 ma). *Palaeoceanography, Palaeoclimatology, Palaeoecology*, *313-314*, 107–126. https://doi.org/10.1029/2003PA000995